Timing of partial melting and granulite formation during the genesis of high to ultra-high temperature terranes: insight from numerical experiments.

Bénédicte Cenki-Tok, Patrice F Rey, Diane Arcay, Julian Giordani

Article type : Research Article

Timing of partial melting and granulite formation during the genesis of high to ultra-high temperature terranes: insight from numerical experiments.

Bénédicte Cenki[1], Patrice F. Rey[2], Diane Arcay[1], and Julian Giordani[2]

[1]*Géosciences Montpellier, Université de Montpellier, CNRS, 34095 Montpellier cedex 5, France ; benedicte.cenki@umontpellier.fr;*

[2]*Earthbyte Research Group, ARC ITRH Basin Genesis Hub, School of Geosciences, University of Sydney, NSW 2006, Sydney, Australia*

Short title: Numerical modelling of the formation of HT-UHT terranes

Significance statement

Even though long-lived high to ultra-high temperature (HT-UHT) terranes which formed mostly during the Proterozoic have been widely studied, their mode of formation is still controversial. We address the intertwined timing of partial melting and granulite formation during the genesis of HT-UHT terranes in a manner that cannot be derived from the natural rocks archive.

This paper is innovative in the sense that it illustrates this problem in a dynamic manner. We illustrate through 2D thermo-mechanical modelling of an orogenic cycle that i) the formation of HT-UHT terranes can be explained by an elevated crustal radiogenic heat production and ii) the timing and duration of partial melting and the formation of granulites (syn-convergence and/or syn-collapse). The numerical modelling code used is the well-tested open-source code *Underworld* (https://www.underworldcode.org) making the results and outcomes reproductible and transparent for the scientific community.

This article has been accepted for publication and undergone full peer review but has not been through the copyediting, typesetting, pagination and proofreading process, which may lead to differences between this version and the Version of Record. Please cite this article as doi: 10.1111/TER.12577

These results have major implications for the understanding of the evolution of continental crusts in general, and for this reason our paper, in addition to be provocative and innovative, will be of very broad interest to the geoscience community.

ABSTRACT

Long-lived high to ultra-high temperature (HT-UHT) granulitic terranes formed throughout Earth's history. Yet, the detailed processes involved in their formation remain unresolved and notably the sequence of appearance and duration of migmatisation and granulites conditions in the orogenic cycle. These processes can be evaluated by analytical and numerical models. Firstly, solving the steady-state heat equation allows to underline the interdependency of the parameters controlling the crustal geotherm at thermal equilibrium. Secondly, performing 2D thermo-mechanical experiments of an orogenic cycle, from shortening to gravitational collapse, allows to consider non steady-state geotherms and understand how deformation velocity may affect the relative timing of migmatite and granulite formation. These numerical experiments with an elevated radiogenic heat production and slow shortening rates allow the formation of large volumes of prograde migmatites and granulites going through the sillimanite field as observed in many HT-UHT terranes. Finally, the interplay between these parameters can explain the difference in predicted Pressure-Temperature-time paths that can be compared with the natural rock archive.

Introduction

High to ultra-high temperature (HT > 650°C, UHT > 900°C) metamorphism plays a key role in the stabilization of continents during orogenesis (Harley, 2016), the formation and preservation of stable crustal roots (Cenki-Tok *et al.*, 2020) and in the formation of supercontinents (Touret *et al.*, 2016). There is a robust record of natural examples documenting the duration of UHT events and their corresponding geodynamic setting (Kelsey and Hand, 2015; Brown *et al.*, 2020). Harley (2016) proposed that "slow" (long-lived) granulites predominantly form in large hot orogens (LHO) as defined by Beaumont et al. (2010) whereas "fast" (short-lived) episodes of granulite-facies metamorphism may be restricted to back-arc settings. However, the respective timing, duration and volume of migmatites and granulites is difficult to extract from the rocks archive. Here, the first part of this study explores the equilibrium thermal state of the continental lithosphere for a broad range of crustal thicknesses (20 to 80 km), and mantle heat flow (4 to 80 $mW.m^{-2}$), radiogenic heat production and crustal differentiation estimated by the ratio between the heat production measured at the surface of the crust and the crustal mean (Perry *et al.*, 2006). Conditions for partial melting and granulite facies may be established for a wide range of crustal thicknesses. However, these conditions which assume thermal equilibrium are unlikely to be achieved as the resulting hot crust would collapse under gravitational deviatoric stresses. Hence, the second part of the paper focusses on 2D thermo-mechanical experiments to constrain the respective tempo of partial melting and granulites formation as well as predict the shape of Pressure-Temperature-time (PTt) paths of particles via modelling of whole orogenic cycles, from shortening to lithospheric mantle thinning and post-orogenic extension. Whilst the establishment of the conditions for partial melting culminates during convergence, granulite facies conditions generally occurs during orogenic collapse.

Migmatite and granulite potential at thermal equilibrium

Neglecting heat advection and heat production in the mantle, the solution of the steady-state heat equation allows for the prediction of the equilibrium geotherm, and therefore the potential for the continental crust to reach HT-UHT conditions. The thermal state of the continental lithosphere at equilibrium depends on i/ the mantle basal heat flow (*BHF*), ii/ the total amount of radiogenic heat production (*RHP*), iii/ its distribution throughout the crust ($H(z)$), iv/ the thermal diffusivity of rocks (κ), and v/ the surface temperature (T_o). For conditions ii to v fixed, the graphs in Figure 1 map the Moho temperature controlled by crustal and lithospheric thicknesses modulated by the

BHF. For a global average 40 km -thick continental crust (Christensen and Mooney, 1995), a *BHF* of 20 mW/m^{-2}, and with an average total *RHP* of 1.0483 μW.m^{-3}, close to present-day values (Taylor and McLennan, 1995), the Moho temperature ranges from 650 °C when the *RHP* distribution is uniform (Fig. 1A) to 575 °C when the crust is differentiated with a length scale factor *hc* of 20 km (i.e., $H(z) = Ho \times exp(-z \times hc)$, where *Ho* and *H(z)* are the heat production at the surface and at depth *z*, respectively Fig. 1B). At this moderate level of *RHP*, continental crusts must achieve a thickness > 70 km to experience granulite facies conditions (purple region in Fig.1). For a higher average total *RHP* of 2.0966 μW.m^{-3}, appropriate for Paleoproteroic to Archean times, the temperature at the Moho reaches 1020ºC for uniform *RHP* distribution in the crust, and 810ºC when the *RHP* decreases exponentially with depth (from 5 μW.m^{-3} at the surface) with *hc* = 20 km. The potential for a 40-km thick crust to reach migmatite and granulite conditions is significantly enhanced (Fig.1 C, D; Vanderhaeghe *et al.*, 2019). However, such high temperatures are unsustainable on long time scales as such a hot crust would collapse, spreading onto adjacent ocean basins (Bailey, 1999). This confirms that the conditions to form significant volumes of HT-UHT rocks can be controlled by the total *RHP* and the degree of differentiation of the continental crust (McLaren *et al.*, 1999; Gerya *et al.*, 2002; Clark *et al.*, 2011; Sandiford and McLaren, 2002, Kelsey and Hand, 2015). In what follows, 2D thermo-mechanical experiments of a complete orogenic cycle allow to explore the additional effect of the tectonic velocities and assess the tempo and duration of migmatitic and granulite conditions.

Numerical experiments, code, and model setup

The numerical models are performed with *Underworld,* a well-tested open-source finite element code, to solve the equations of conservation of momentum, mass and energy for an incompressible fluid on a Cartesian Eulerian mesh (Moresi *et al.*, 2002, 2003, 2007; Beucher *et al.*, 2019; Mansour *et al.*, 2020). The 2D thermo-mechanical experiments involve a geological model of dimension 480 km x 160 km discretized over a computational grid made of 240 x 80 elements. The initial set up consists of a 35 or 40 km thick crust with 20 km air-like material above, and mantle below (Fig. 2A-B). Each model runs through three stages: i) a shortening phase during which the crust thickens to ~ 60 km with either a slow total velocity of 0.24 cm.y^{-1} during 70 My or a fast total velocity of 2.4 cm.y^{-1} during ~ 7 My (delivering a strain rate averaged over the length of the model of 1.6 x 10^{-16} s^{-1} and 1.6 x 10^{-15} s^{-1} respectively); ii) a rapid increase in *BHF* (from 0.020 W.m^{-2} to 0.030 W.m^{-2}) over 2.5 My while the velocities imposed on the vertical

boundaries are set to zero (v_x = v_y = 0 cm.y^{-1}), mimicking the thermal impact of a mantle delamination phase; iii) a relaxation phase in which the crust returns to normal thickness, under slow extensional boundary conditions (total velocity of 0.10 cm.y^{-1}) associated to a decrease in *BHF* from 0.030 W.m^{-2} to 0.020 W.m^{-2} in ~ 70 My. Details of modeling procedures, rheological and thermal parameters as well as the input python script are available as supplementary data.

The data that supports the findings of this study are available in the supplementary material of this article

These experiments focus on two end-member crustal structures with average values of total *RHP* at ~ 1 and ~ 2 μW.m^{-3} (Fig. 2). A value of ~ 1 μW.m^{-3} is in line with *RHP* calculation predicted from the present-day composition of the bulk continental crust determined by Taylor and McLennan (1995). Models *RHP1_unif* mimic a Phanerozoic orogenic cycle involving a continental crust with a uniform *RHP* (1.0483 μW.m^{-3}), yielding an initial Moho temperature of 650°C at 40 km depth (Fig. 1A). However, Mareschal and Jaupart (2013), Artemieva *et al.* (2017) and Gard *et al.* (2019) showed that the crustal *RHP* may have been higher than 1 μW.m^{-3} during the Proterozoic, having varied between 0.8 and 4 μW.m^{-3} between 0.5 and 2.5 Ga with an average *RHP* close to ~ 2 μW.m^{-3}. In addition, recent studies reveal that, in tectonically stable regions, the upper crust's *RHP* may be higher than in the lower crust (Goes *et al.*, 2020; Alessio *et al.*, 2020). The conditions for model *RHP2_diff* include a total average *RHP* of 2.0922 μW.m^{-3} with high *RHP* in the upper crust (5 μW.m^{-3}) that decreases exponentially with a length scale factor *hc* of 20 km, yielding an initial Moho temperature at 35 km depth of 650°C (Fig. 1D). Models *RHP2_diff* aim at approaching thermal conditions of a differentiated crust prevailing during the Proterozoic.

Results

Despite similar initial Moho temperatures (~ 650 °C), the two experiments show very different thermal evolutions. In models *RHP2_diff* the production of migmatites occurs at the onset of crustal thickening (Fig. 3A, C). This contrasts with models *RHP1_unif,* in which the conditions for migmatites appear after a few 10's of My of crustal thickening (Fig. 3B, D). Granulite conditions generally appear a few 10's of My after the onset of migmatisation but the bulk of granulite formation occurs during the post-convergence collapse phase (Fig. 3A, B, C). Model *Slw_RHP2_diff* (Fig. 2C-D, 3A) allows for the prograde formation of granulites and migmatites reaching a uniform 20 km-thick granulite facies lower crust and a 20 km-thick migmatitic layer on

top at the end of the shortening phase (Fig. 2C). At the end of the experiment, the temperature at the Moho reaches UHT conditions (Fig. 3A, 4A). The thickness of the HT-UHT crust is only slightly reduced after the relaxation phase (Fig. 2D). Note that the unmetamorphosed upper crust has thinned to 15 km after the relaxation phase assisted by erosion. Model *Fst_RHP2_diff* (Fig. 2G-H, 3C) does not show the formation of granulites during shortening and delamination and only a very low degree of partial melting in a large volume of crust (Fig. 2G). It is only at a late orogenic stage, during collapse, that the crust is hot enough to generate granulites (Fig. 2H, 3C). Model *Slw_RHP1_unif* (Fig. 2E-F, 3B) allows the local formation of a granulite-cored migmatitic dome but there is no pervasive formation of HT rocks in the crust at the end of the shortening phase (Fig. 2E). Through gravitational collapse, a ~10-15 km thick layer of partially molten rocks and a thin ~ 5-10 km granulitic layer form (Fig. 2F, 3B). Model *Fst_RHP1_unif* (Fig. 2I-J, 3D) does not lead to the prograde formation of granulite and/or migmatites during shortening (Fig. 2I). It is only when the crust is thermally relaxed, that the lower crust becomes partially molten (Fig. 2J), but granulites do not form (Fig. 3D).

Figure 4 shows that PTt paths are mainly clockwise, with prograde paths showing gentle slopes for slow shortening velocity (Fig. 4A, C), and steeper slopes for fast shortening velocity (Fig 4B, D). For the *RHP2_diff* models, the upper crust records PTt histories involving isobaric heating then cooling across the andalusite and sillimanite fields (Fig. 4A, B), whereas the middle and lower crust start in the stability field of kyanite and evolve into the sillimanite field (Fig. 4A, B). This strongly contrasts with models *RHP1_unif,* in which the continental crust remains in the kyanite stability field (Fig. 4C, D). Particles generally reach their peak temperature 40 to 60 My after collapse has begun and stay at HT for at least 10 to 15 My. However, PTt paths in model *Fst_RHP2_diff* (Fig. 4B) are more complex and record a short (a few My) near peak P isothermal heating phase before a decompression and cooling path. Interestingly, in models *RHP2_diff* (Fig. 4A, B), particles starting in the upper half of the crust (< 15 km) rather record near-isobaric heating followed by near-isobaric cooling.

Discussion and conclusions

In these numerical experiments, prograde granulites evolving through the sillimanite field, similar to many HT-UHT terranes (Fig. 4E), form when shortening velocities are slow and *RHP* is high (*Slw_RHP2_diff*, Fig. 2C-D, 3A, 4A). In most cases, the formation of granulites is a late orogenic process starting *ca.* 8 to 20 My after collapse has begun (Fig. 3B-C, 4B-C). Granulites can be very

localized in the deep crust as in *Slw_RHP1_unif* (Fig. 2E-F, 3B). This case highlights another way to form localized granulites in addition to the back-arc geodynamic settings suggested by Harley (2016). This model may be an analogue for the Variscan crust, dominated by partially molten products (Lardeaux, 2014) in which the lower crust records an episode of late orogenic granulites documented in xenoliths (310-290 Ma, Costa and Rey, 1995; Puelles *et al.*, 2019). In the Variscan belt, km-size lenses of granulites can be found in the Alps (Gruf Complex, Galli *et al.*, 2012), in the Pyrenees (Agly charnockite, Odlum *et al.*, 2019) or in migmatitic domes of the Bohemian Massif (Lexa *et al.*, 2011; Maierovà *et al.*, 2014). The peak PTt conditions and PT path shapes for granulites (Fig. 4) are in agreement with the parametric study for different tectonic units of the Bohemian Massif that reflects a large variability in total *RHP* and shortening velocities (Maierovà *et al.*, 2014).

Finally, the formation of long-lived regional scale HT-UHT rocks, ubiquitous through Earth history (Harley, 2016; Fitzimmons, 2016) and generally associated with large hot orogens (Beaumont *et al.*, 2010), is best explained by the model *Slw_RHP2_diff*. It is characterized by a differentiated shallow crust enriched in radiogenic elements and undergoing slow shortening rates. Migmatites form throughout the orogenic cycle and granulites form mainly during the collapse phase (Fig. 2C-D, 3A, 4A). These terranes typically record HT-UHT metamorphism with retrograde near-isothermal decompression paths (Fig. 4E) as predicted in *Slw_RHP2_diff* (Fig. 4A). Similarly, models for the Grenville orogen (Jamieson *et al.*, 2010) present PTt paths for particles starting in the lower crust with a steep prograde burial path, followed by isothermal decompression, culminating at ~ 14 kbar and ~ 950 °C (Fig. 4E) that is in line with the rock archive. Other granulitic terranes present near-isothermal decompression paths culminating at 8 – 13 kbar and 900 - 1000°C depending on the starting depth of the particles (Fig. 4E; In Ouzzal, Algeria; Mather gneisses, Antarctica; Palni Hills, India; references in Harley, 2016). Interestingly, particles starting in the upper crust for models *RHP2_diff* and independent of the shortening velocity (Fig. 4A, B), present isobaric heating-cooling path similar to migmatitic terranes like, for example, southern India that records UHT melt-producing and melt-consuming steep reactions (Cenki *et al.*, 2002). Finally, the interplay between total *RHP*, its distribution and shortening velocities can explain PTt paths for dominantly granulitic or migmatitic terranes as well as differences in the relative tempo of formation of migmatites and granulites during the orogenic cycle (syn-convergence and/or syn-collapse) which is not accessible from the natural rock archive.

Acknowledgements

We acknowledge the funding from the European Union's Horizon 2020 research and innovation program under grant agreement No 793978. This research was undertaken with the assistance of resources from the National Computational Infrastructure (NCI), through the National Computational Merit Allocation Scheme supported by the Australian Government; the Pawsey Supercomputing Centre with funding from the Australian Government and the Government of Western Australia, and support from the Australian Research Council grants ARC-IH130200012 and ARC-LP190100146. We thank R. Beucher for his expert support with *Underworld*, M. Hand and F. Garel for constructive discussions, an anonymous reviewer and K. Mezger for editorial handling.

References

Alessio, K.L., Hand, M., Hasterok, D., Morrissey, L.J., Kelsey, D.E., and Raimondo, T., 2020. Thermal modelling of very long-lived (> 140 Myr) high thermal gradient metamorphism as a result of radiogenic heating in the Reynolds Range, central Australia. *Lithos*, **352**, 105280.

Artemieva, I.M., Thybo, H., Jakobsen, K., Sørensen, N.K., and Nielsen, L.S., 2017. Heat production in granitic rocks: Global analysis based on a new data compilation GRANITE2017. *Earth-Science Reviews*, **172** (Supplement C), 1–26.

Bailey, R., 1999. Gravity-driven continental overflow and Archaean tectonics. *Nature*, **398**, 413-415.

Beaumont, C., Jamieson, R.A., and Nguyen, M.H., 2010. Models of large hot orogens containing a collage of reworked and accreted terranes. *Canadian Journal of Earth Sciences*, **47**, 485– 515.

Beucher, R., Moresi, L., Giordani, J., Mansour, J., Sandiford, D., Farrington, R., Mondy, L., Mallard, C., Rey, P., Duclaux, G., Kaluza, O., Laik, A., and Morón, S., 2019. UWGeodynamics: A teaching and research tool for numerical geodynamic modelling. *Journal of Open Source Software*, **4(36)**, 1136.

Brown, M., Kirkland, C.L., and Johnson, T.E., 2020. Evolution of geodynamics since the Archean: Significant change at the dawn of the Phanerozoic. *Geology*, **48**, 488–492.

Cenki, B., Kriegsman L.M., and Braun I., 2002. Melt-producing and melt-consuming reactions in the Achankovil cordierite gneisses, South India. *Journal of Metamorphic Geology*, **20**, 543-561.

Cenki-Tok, B., Rey, P. F., and Arcay, D., 2020. Strain and retrogression partitioning explain long-term stability of crustal roots in stable continents. *Geology*, **48(7)**, 658-662.

Christensen, N.I., and Mooney, W.D., 1995. Seismic velocity structure and composition of the continental crust: A global view. *Journal of Geophysical Research*, **100**, 9761-9788.

Clark, C., Fitzsimons, I.C.W., Healy, D., and Harley, S.L., 2011. How does the continental crust get really hot? *Elements*, **7**, 235–240.

Costa, S. and Rey, P. F., 1995. Lower crustal rejuvenation and crustal growth during post-thickening collapse: Insights from a crustal cross section through a metamorphic core complex. *Geology*, **23**, 905-908.

Fitzsimons, I.C.W., 2016. Pan–African granulites of Madagascar and southern India: Gondwana assembly and parallels with modern Tibet. *Journal of Mineralogical and Petrological Sciences*, **111**, 73–88.

Galli, A., Le Bayon, B., Schmidt, M. W., Burg, J.-P., Reusser, E., Sergeev, S. A., and Larionov, A., 2012. U–Pb zircon dating of the Gruf Complex: disclosing the late Variscan granulitic lower crust of Europe stranded in the Central Alps. *Contributions to Mineralogy and Petrology*, **163**, 353–378.

Gard, M., Hasterok, D., Hand, M., and Cox, G., 2019. Variations in continental heat production from 4 Ga to the present: Evidence from geochemical data. *Lithos*, **342-343**, 391-406.

Gerya, T.V., Perchuk, L.L., Maresch, W.V., Willner, A.P., Van Reenen, D.D., and Smit, C.A., 2002. Thermal regime and gravitational instability of multi-layered continental crust: implications for the buoyant exhumation of high-grade metamorphic rocks. *European Journal of Mineralogy*, **14**, 687-699.

Goes, S., Hasterok, D., Schutt, D.L., and Klöcking, M., 2020. Continental lithospheric temperatures: A review. *Physics of the Earth and Planetary Interiors*, 106509.

Harley, S. L., 2016. A matter of time: The importance of the duration of UHT metamorphism. *Journal of Mineralogical and Petrological Sciences*, **111**, 50-72.

Jamieson, R.A., Beaumont, C., Warren, C.J., and Nguyen, M.H., 2010. The Grenville Orogen explained? Applications and limitations of integrating numerical models with geological and geophysical data. *Canadian Journal of Earth Sciences*, **47**, 517-539.

Kelsey, D. E., and Hand, M., 2015. On ultrahigh temperature crustal metamorphism: Phase equilibria, trace element thermometry, bulk composition, heat sources, timescales and tectonic settings. *Geosciences Frontiers*, **6**, 311-356.

Lardeaux, J.M., 2014. Deciphering orogeny: a metamorphic perspective Examples from European Alpine and Variscan belts. *Bulletin de la Société Géologique de France*, **185(5)**, 281–310.

Lexa, O., Schulmann, K., Janoušek, V., Štipskà, P., Guy, A., and Racek, M., 2011. Heat sources and trigger mechanisms of exhumation of HP granulites in Variscan orogenic root. *Journal of Metamorphic Geology*, **29**, 79-102.

Mansour, J., Giordani, J., Moresi, L., Beucher, R., Kaluza, O., Velic, M., Farrington, R., Quenette, S., and Beall, A., 2020. Underworld 2 : Python geodynamics modelling for desktop, HPC and cloud. *Journal of Open Source Software*, **5(47)**, 1797.

Maierovà, P., Lexa, O., Schulmann, K., and Štipskà, P., 2014. Contrasting tectono-metamorphic evolution of orogenic lower crust in the Bohemian Massif : A numerical model. *Gondwana Research*, **25**, 509-521.

Mareschal, J.-C., and Jaupart, C., 2013. Radiogenic heat production, thermal regime and evolution of continental crust. *Tectonophysics*, **609**, 524-534.

McLaren, S., Sandiford, M., and Hand, M., 1999. High radiogenic heat–producing granites and metamorphism—An example from the western Mount Isa inlier, Australia. *Geology*, **27(8)**, 679-682.

Moresi, L., Dufour, F., and Muhlhaus, H.B., 2002. Mantle convection modeling with viscoelastic/brittle lithosphere: Numerical methodology and plate tectonic modelling. *Pure And Applied Geophysics*, **159(10)**, 2335–2356.

Moresi, L., Dufour, F., and Muhlhaus, H.B., 2003. A Lagrangian integration point finite element method for large deformation modeling of viscoelastic geomaterials. *Journal of Computational Physics*, **184(2)**, 476–497.

Moresi, L., Quenette, S., Lemiale, V., Meriaux, C., Appelbe, B., and Mühlhaus, H.B., 2007. Computational approaches to studying non-linear dynamics of the crust and mantle. *Physics of the Earth and Planetary Interiors*, **163**, 69–82.

Odlum, M.L., and Stockli, D.F., 2019. Thermotectonic Evolution of the North Pyrenean Agly Massif During Early Cretaceous Hyperextension Using Multi-mineral U-Pb Thermochronometry. *Tectonics*, **38(5)**, 1509-1531.

Perry, H.K.C., Jaupart, C., Mareschal, J.-C., and Bienfait, G., 2006. Crustal heat production in the Superior Province, Canadian Shield, and in North America inferred from heat flow data. *Journal of Geophysical Research — Solid Earth*, **111**, B04401.

Puelles, P., Ibarguchi, J.I.G., García de Madinabeitia, S., Sarrionandia, F., Carracedo-Sánchez, M., and Fernández-Armas, S., 2019. Granulite-facies gneisses and meta-igneous xenoliths from the Campo de Calatrava volcanic field (Spain): Implications for the tectonics of the Variscan lower crust. *Lithos*, **342-343**, 114-134.

Sandiford M., and McLaren S., 2002. Tectonic feedback and the ordering of heat producing elements within the continental lithosphere. *Earth and Planetary Sciences Letters*, **204 (1-2)**, 133-150.

Taylor, S.R., and McLennan, S.M., 1995. The geochemical evolution of the continental crust. *Reviews of Geophysics*, **33**, 241–265.

Touret, J. L. R., Santosh, M., and Huizenga, J.M., 2016. High-temperature granulites and supercontinents. *Geosciences Frontiers*, **7**, 101-113.

Vanderhaeghe, O., Guergouz, C., Fabre, C., Duchêne, S., and Baratoux, D., 2019. Secular cooling and crystallization of partially molten Archaean continental crust over 1 Ga. *Comptes rendus – Geoscience*, **351**, 562-573.

Figure caption

Figure 1. Map of the balance at thermal equilibrium for a high (2.0966 μW.m^{-3}) or moderate *RHP* (1.0483 μW.m^{-3}) between crustal thickness (*zc*, x-axis), lithospheric thickness (*zl*, y-axis), basal heat flow *BHF* (light blue lines) and the Moho temperature (dashed orange lines). We set κ = 9 10^{-7} m^2.s^{-1} and T_o = 25°C. Pink dots indicate the chosen initial conditions, blue dots indicate conditions for a 40 km thick crust. The grey domain represents predicted z_c-z_l combinations. The pink and yellow regions represent crustal domains where granulite and migmatite are stable, respectively.

Figure 2. A-B. Model geometry, initial conditions as well as geotherm, viscosity and density profiles. The circles pattern superimposed on the continental crust represents the finite strain ellipses. White squares represent the Lagrangian particles recording the PTt paths presented in Fig. 4. A. Initial conditions for models *RHP2_diff*, mimicking a Proterozoic highly differentiated and highly radiogenic crust. B. Initial conditions for model *RHP1_unif*, simulating a Phanerozoic uniform and less radiogenic crust. C-J. Orogenic modeling results showing two snapshots for each model: i) shortening-delamination and ii) collapse. Shortening velocity is either slow (0.24 cm.y^{-1}, C-F) or fast (2.4 cm.y^{-1}, G-J).

Figure 3. Depth – time profiles indicating the onset of partial melting and granulite formation through the evolution of the models presented in Fig. 2.

Figure 4. A-D. PTt paths for all particles (light grey background) shown on Fig. 2. The PTt paths for the particles initially located in the center of the model are highlighted in dark grey. As a reference, the stability field for aluminosilicates and the crustal melting domains (pink) are represented. Horizontal triangles pinpoint the onset (in My) of melt (purple) and granulite (brown) formation. E. Selected representative PT path for natural analogues.

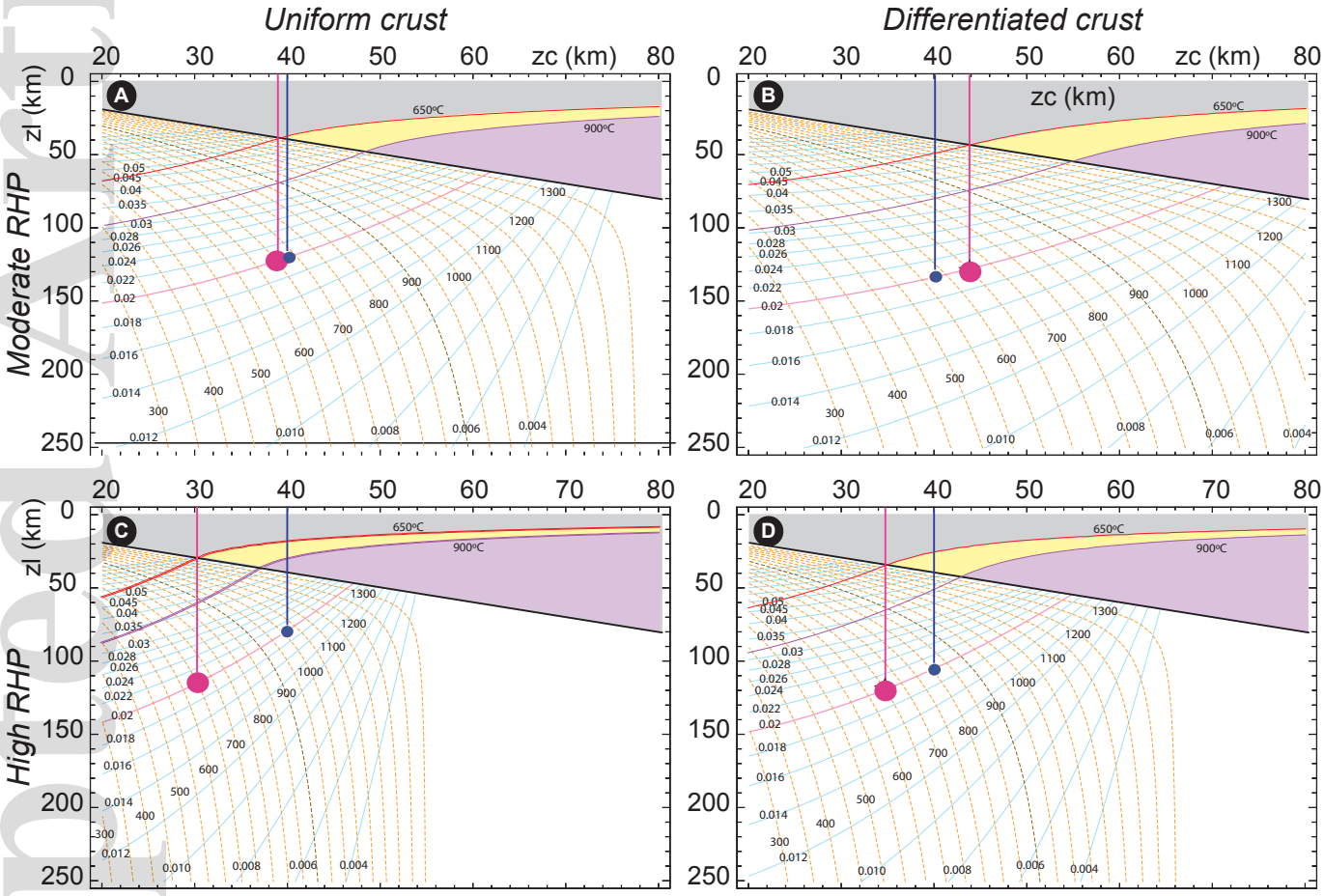

Figure 1

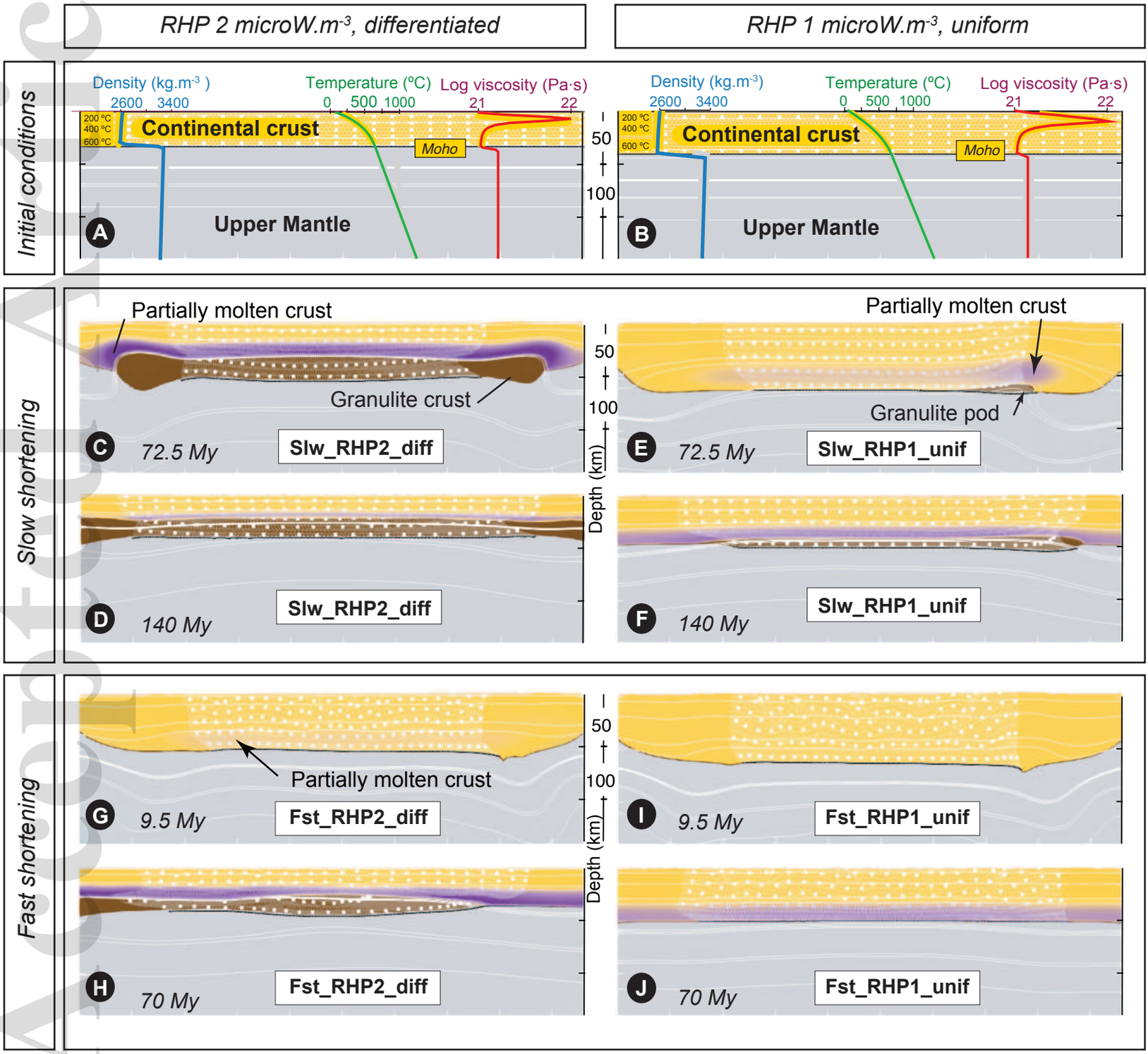

Figure 2

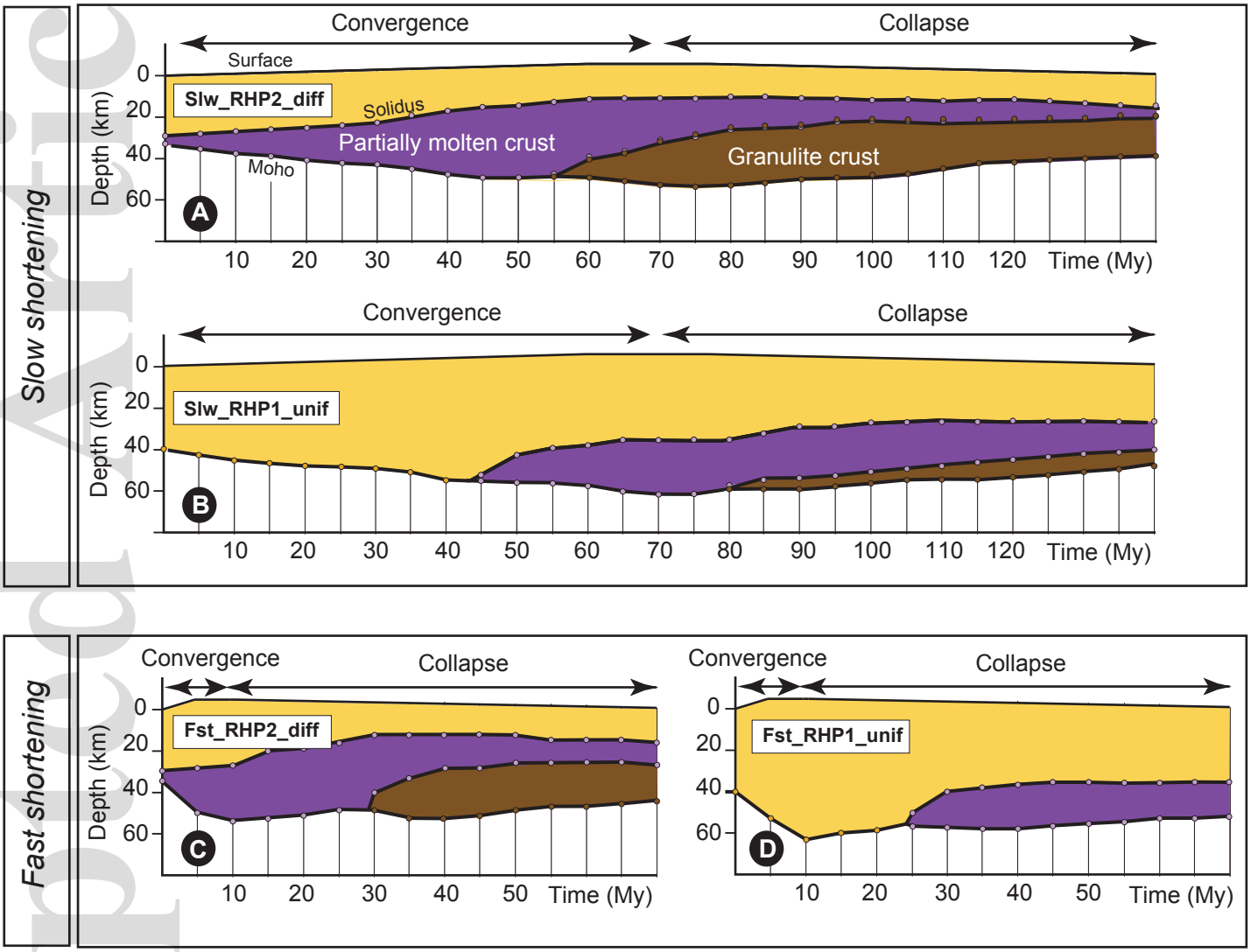

Figure 3

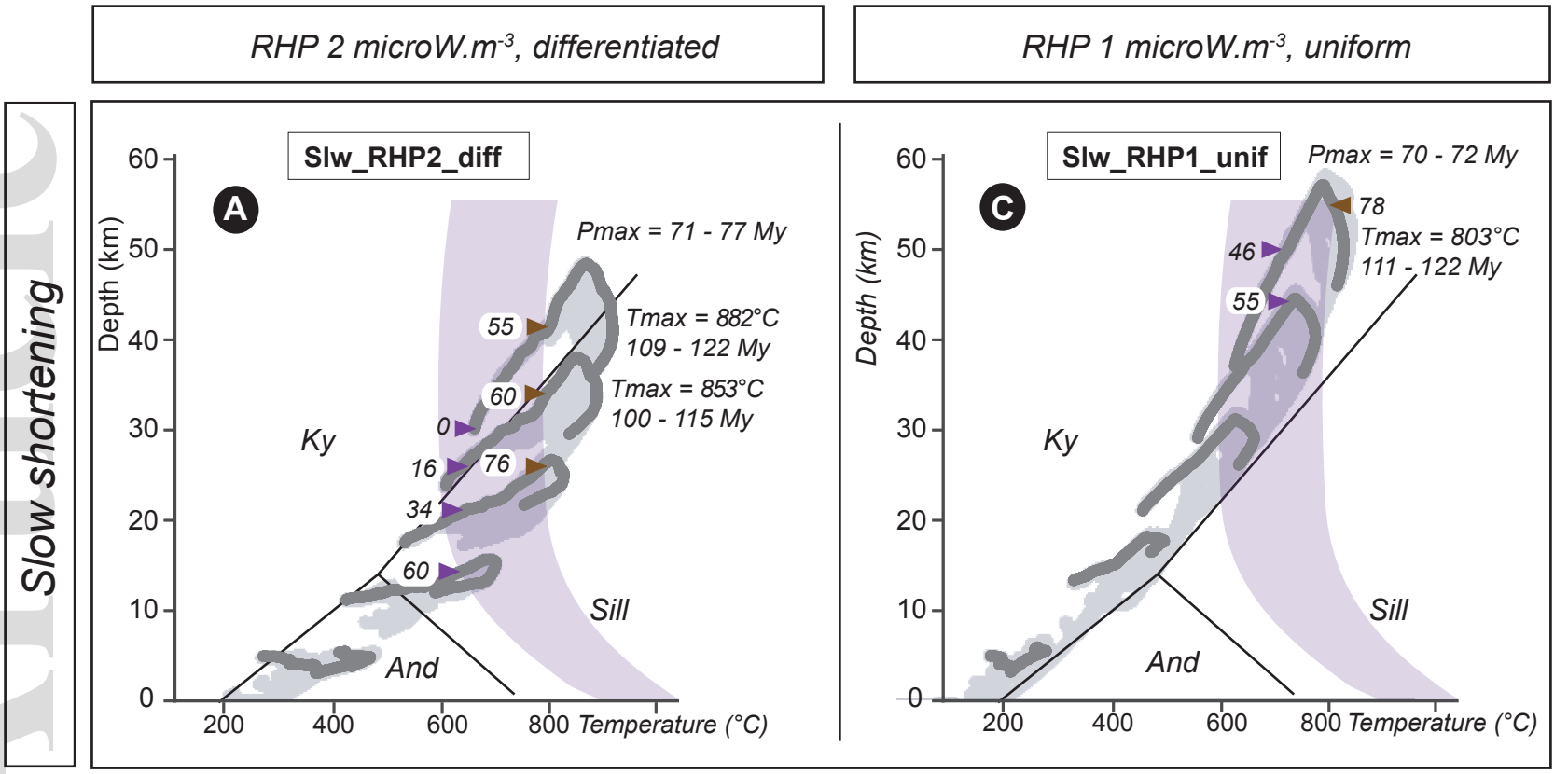

Figure 4

Gre: Grenville model (Jamieson et al., 2010)

Ouz: In Ouzzal
Mat: Mather gneisses
Pal: Palni Hills
(refs. in Harley, 2016)

Sgt: southern India (Cenki et al., 2002)

Figure caption

Figure 1. Map of the balance at thermal equilibrium for a high (2.0966 μW.m^{-3}) or moderate *RHP* (1.0483 μW.m^{-3}) between crustal thickness (*zc*, x-axis), lithospheric thickness (*zl*, y-axis), basal heat flow *BHF* (light blue lines) and the Moho temperature (dashed orange lines). We set κ = 9 10^{-7} m^2.s^{-1} and T_o = 25°C. Pink dots indicate the chosen initial conditions, blue dots indicate conditions for a 40 km thick crust. The grey domain represents predicted z_c-z_l combinations. The pink and yellow regions represent crustal domains where granulite and migmatite are stable, respectively.

Figure 2. A-B. Model geometry, initial conditions as well as geotherm, viscosity and density profiles. The circles pattern superimposed on the continental crust represents the finite strain ellipses. White squares represent the Lagrangian particles recording the PTt paths presented in Fig. 4. A. Initial conditions for models *RHP2_diff*, mimicking a Proterozoic highly differentiated and highly radiogenic crust. B. Initial conditions for model *RHP1_unif*, simulating a Phanerozoic uniform and less radiogenic crust. C-J. Orogenic modeling results showing two snapshots for each model: i) shortening-delamination and ii) collapse. Shortening velocity is either slow (0.24 cm.y^{-1}, C-F) or fast (2.4 cm.y^{-1}, G-J).

Figure 3. Depth – time profiles indicating the onset of partial melting and granulite formation through the evolution of the models presented in Fig. 2.

Figure 4. A-D. PTt paths for all particles (light grey background) shown on Fig. 2. The PTt paths for the particles initially located in the center of the model are highlighted in dark grey. As a reference, the stability field for aluminosilicates and the crustal melting domains (pink) are represented. Horizontal triangles pinpoint the onset (in My) of melt (purple) and granulite (brown) formation. E. Selected representative PT path for natural analogues.